



## Fabrication of a Staircase Coil with Improved SNR and Image Uniformity by Structural Changes of a Conventional Birdcage Coil at 1.5T MRI

Kyung-Seung Ryang\*, Yong-Jin Shin

Div. of Physics and Chemistry, Natural Science College of Chosun University, Gwangju, Korea.

Received February 10, 2003

**Abstract** : The performance of radio frequency (RF) coils, used in MRI units, is determined by the image uniformity and the signal-to-noise ratio (SNR). Birdcage and surface coils are commonly used. A birdcage coil provides a good image uniformity while a surface coil produces a high SNR. In this study, therefore, a staircase coil was designed from a standard version of a birdcage coil, with some structural changes to increase SNR while maintaining image uniformity. In phantom experiments, the improvement of the image to uniformity and the SNR increase of the staircase coil compared with the values for the birdcage coil were about 3.5% and 35%, respectively. In clinical experiment, the SNR increase of the staircase coil, compared with the value for the birdcage coil was about 40% in bone, muscle and blood-vessel tissues. These results show that the performance of the staircase coil was very improved over the standard birdcage coil in terms of SNR, and that image uniformity was maintained. Therefore, the staircase coil designed by this study should be useful in experimental and clinical 1.5T MRI systems, and this coil offers an alternative method of quadrature detection.

Key words: SNR; image uniformity; staircase coil; quadrature detection

### INTRODUCTION

One of the most important elements of the magnetic resonance imaging system is radio frequency (RF) coil, which is used to transmit and receive electromagnetic energy of given nuclear Larmor frequency. The RF coils, commonly used in modern MRI units are birdcage and surface coils, and the performance of these coils is determined by image uniformity and the signal-to-noise ratio (SNR) factor. A birdcage coil provides good image uniformity while a surface coil produces a high SNR.<sup>1-4</sup> Therefore, the optimum coil has close to the image

\* To whom correspondence should be addressed. E-mail: ksr7453@chosun.ac.kr

uniformity of a birdcage coil and the SNR of a surface coil. Conventional clinical MRI systems are used at an external static magnetic field of 1.5T, but in the case of the need for high sensitivity, high magnetic fields are used. Higher static magnetic field strength can increase the sensitivity of MRI and spectroscopy studies. However, the higher the external static magnetic field, the harder it is to obtain magnetic field uniformity in the sample. In addition, because of the increase in the amount of RF absorbed by the sample, the SAR (specific absorption rate) becomes a topic of concern.

In this study, we evaluated a staircase coil with good image uniformity and the high SNR at a relatively low 1.5T external static magnetic field.<sup>5-12</sup> For the resonance theory, real and imaginary components of signal were produced inside the loop type coil such as a birdcage. In general, a quadrature coil, which was separated 90 degrees, was used for detection of these signals simultaneously. For the acquisition of the two components of signals, a new type coil was fabricated using a stepped leg, not a straight or spiral type coil. And the coil was designed from the standard version of a birdcage coil, whilst maintaining image uniformity, and then applied with some structural changes to increase the SNR. Instead of straight axial conductors, the staircase coil uses the same length stepped conductors. And, for the equal leg spacings and the coil length, each coil leg was rotated with  $3\pi/4$  rotation angle in the same direction. This rotation angle was optimally determined from the repeated experiment at various angles. Because the coil preserves discrete rotational symmetry around the axes, it should produce modes with sinusoidal current distributions much like the birdcage coil.<sup>13-15</sup> Birdcage and staircase coils are fabricated and then tested in linear operation mode.

## MATERIALS AND METHODS

### *Fabrication*

High pass birdcage and staircase coils were constructed on an acrylic plastic cylinder of outside diameter 12cm and length 19cm. We used thin copper adhesive tapes for endings and legs, 13mm and 5mm in width, respectively. Endings were cut at 2mm and connected with seven 38mm size chip capacitors (American Technical Ceramics, Huntington Station, New York, USA). For the transmission and reception of RF, the coil was suspended from a coaxial cable of 50Ω impedance. In the birdcage coil, eight straight axial legs were mounted on a rigid plastic with angular spacings of  $\pi/4$  radians. The legs were individually soldered to the upper and lower endings outside the plastic cylinder. In the staircase coil, eight legs were mounted to form a staircase on a rigid plastic with angular spacings of  $\pi/4$  radians, the total angle spanned by each leg was  $3\pi/4$  radians.

Table 1. Experimental result of frequency tuning and impedance matching of 8 leg high pass birdcage and staircase coils during unloading and phantom loading.

Coil type	Resonance frequency tuning (MHz)		Impedance matching value (dB)	
	Unloading	Phantom loading	Unloading	Phantom loading
Birdcage coil	63.7	63.7	-8	-24
Staircase coil	63.7	63.9	-12	-26

### *Determination of Resonant Modes*

Frequency and impedance measurements were obtained using an Anritsu Wiltron network analyzer (40M - 3GHz, Japan). Birdcage and staircase coils were tuned for proton resonant frequency on a 1.5T General Electric MRI system operating at 63.87MHz and matched to an impedance of 50  $\Omega$ . Tuning and matching experiment was performed in unloading and phantom (10mM CuSO<sub>4</sub>) loading. Values of the tuning frequency and of the matching impedance of these coils are shown in Table 1. Pictures of the constructed coils are shown in Fig. 1.

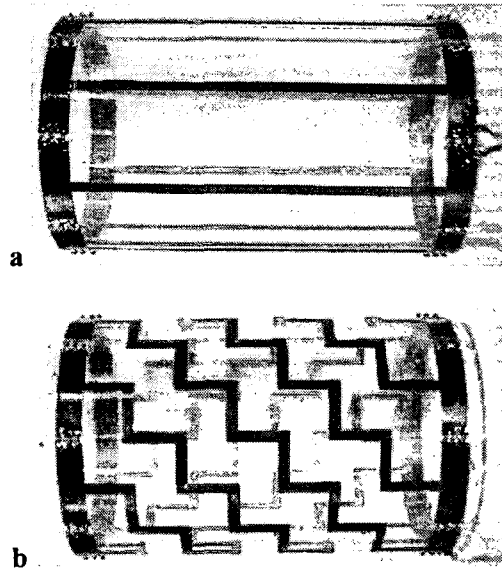


Fig. 1. Pictures of the constructed 8 legs high pass coil. a) Birdcage coil and b) staircase coil of 120mm diameter.

### Measurement Methods

Image of the 10mM CuSO<sub>4</sub> phantom 6cm in diameter, and a wrist joint were obtained using widely used clinical MRI (GE, Signa Horizon, U.S.A.) at a magnetic field of 1.5T. Image uniformity and SNR were measured from the imaging space of the phantom, and only SNR values were measured from the imaging space of the wrist joint in the IDL program. Image uniformity was calculated using by:

$$Uniformity = \left[ 1 - \frac{S_{max} - S_{min}}{S_{max} + S_{min}} \right] \times 100\% \quad [1]$$

where  $S_{max}$  and  $S_{min}$  are, respectively, the maximum and minimum values of the signal intensity measured in the image of phantom and wrist joint. And SNR was calculated using by:

$$SNR = \frac{S_{avg} - N_{avg}}{N_{std}} \quad [2]$$

where  $S_{avg}$  is the average value signal intensity of the no structure slice phantom image and the tissue of wrist joint of the image,  $N_{avg}$  and  $N_{std}$ , respectively, are the average value signal intensity and the standard deviation of no structure slice phantom image and of the wrist joint of the image.

## RESULTS

### Phantom Experiment

Phantom experiments were conducted using a prototype birdcage and staircase coil developed for clinical MRI. We used a uniform cylindrical phantom (diameter 6cm) filled with CuSO<sub>4</sub> doped distilled water. Fig. 2 displays the axial original images of the phantom acquired using these coils. These images were taken using a fast spin-echo sequence with a pulse repetition time (TR) of 3000ms, a echo time (TE) of 15ms, a flip angle of 90°, a bandwidth of 16kHz, a field of view (FOV) of 16cm×16cm, a thickness of 5.0mm, a matrix of 256×192, and a 1 number of excitation (NEX). Acquired images were sent to a workstation (Sun SPARC) and analyzed using IDL (The Interactive data language, Research Systems, Inc.) program. Histograms of each original image were calculated from a full region containing the image of the sample, as shown in Fig. 3, and image uniformity and SNR values were calculated from the original images of the phantom acquired using birdcage and staircase coils as shown in Table 2. Table 2 shows the image uniformity and SNR calculated from the image of the phantom and the transmitter gain values acquired in the pre-scan mode of MRI scanner.

In phantom experiments, image uniformity and SNR ratio increases of the staircase coil

against the birdcage coil were about 3.5% and 35%, respectively. Therefore, these results showed that the performance of the staircase coil was better than the birdcage coil.<sup>15</sup>

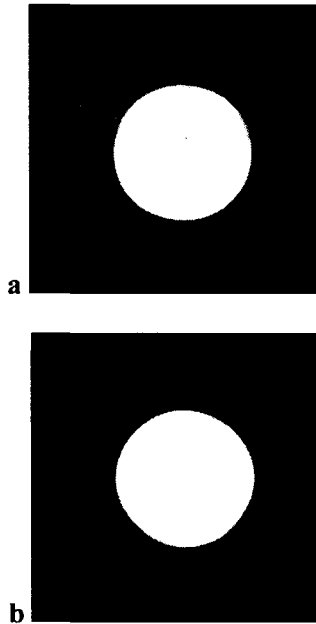


Fig. 2. Original axial images of the phantom 6cm in diameter. a) Birdcage coil and b) staircase coil.

### Clinical Experiment

The performance increment of the staircase coil was determined using the phantom experiment. This was confirmed by performing a clinical experiment on a wrist joint under the same conditions. Sagittal  $T_1$ -weighted images were taken using a fast spin-echo sequence with the following imaging parameters: TR = 3000ms, TE = 98ms, flip angle =  $90^\circ$ , a 16kHz bandwidth, a  $16\text{cm} \times 16\text{cm}$  FOV, thickness = 3mm, and a  $256 \times 192$  matrix. Sagittal  $T_2$ -weighted images were taken using a spin-echo sequence with the following imaging parameters: TR = 450ms, TE = 9ms, flip angle =  $90^\circ$ , a 16kHz bandwidth, a  $16\text{cm} \times 16\text{cm}$  FOV, thickness = 3mm, and a  $256 \times 192$

matrix. Axial images was taken using a gradient-echo sequence with the following imaging parameters: TR = 450ms, TE = 18ms, flip angle = 20°, a 16kHz bandwidth, a 15cm×15cm FOV, thickness = 4mm, and a 256×192 matrix. Sagittal T<sub>1</sub>-weighted, T<sub>2</sub>-weighted images and gradient echo axial images acquired using the birdcage and staircase coils are shown in Figs. 4, 5, and 6, respectively. Signal and noise values measured from the tissues in sagittal and axial images are shown in Tables 3 and 4, respectively, and calculated SNR values for the tissues are shown in Table 5.

In clinical experiments, the SNR of the staircase coil was 39~42% higher than the birdcage coil in T<sub>1</sub>-weighted images, 42~48% in T<sub>2</sub>-weighted images and 52~80% in gradient echo images.

Table 2. Image uniformity and SNR values calculated from the image of the phantom acquired using a birdcage and a staircase coil.

Coil type	Uniformity (%)	SNR
Birdcage coil	87	128
Staircase coil	90	173

Table 3. Signal and noise values measured from the T<sub>1</sub>-weighted and T<sub>2</sub>-weighted sagittal images

	Tissue	Birdcage coil		Staircase coil	
		T <sub>1</sub> image	T <sub>2</sub> image	T <sub>1</sub> image	T <sub>2</sub> image
Signal Value	Bone	584.7	373.8	767.7	522.7
	Muscle	187.9	69.2	238.4	95.3
Noise Value	Mean	12.8	13.7	11.9	13.4
	Standard deviation	8.6	7.0	8.0	7.0

Table 4. Signal and noise values measured from the gradient echo axial images

	Tissue	Birdcage coil	Staircase coil
Signal value	Bone	166.5	206.5
	Muscle	83.0	106.5
	Blood vessel	307.0	350.0
Noise value	Mean	11.6	8.7
	Standard deviation	5.8	4.4

Table 5. Calculated SNR values for the tissues of the wrist joint

Image	Tissue	Birdcage coil	Staircase coil
T <sub>1</sub> sagittal	Bone	66.5	94.5
	Muscle	20.4	28.3
T <sub>2</sub> sagittal	Bone	51.4	72.8
	Muscle	7.9	11.7
GRE axial	Bone	26.7	45.0
	Muscle	12.3	22.2
	Blood vessel	50.9	77.6

### DISCUSSION

Using the conventional 8 leg high pass type birdcage and staircase coils, comparative experiments of the coil performance were performed upon a phantom and a wrist joint. In phantom experiments, the image uniformity of the birdcage and staircase coils was 87% and 90%, and the SNRs were 128 and 173, respectively. Therefore, image uniformity and SNR increment ratio for the staircase coil versus the conventional birdcage coil were about 3.5% and 35%, respectively. Also, these performance increments were shown in clinical experiments. SNR increment ratio for the staircase coil against the conventional birdcage coil were about 40% in T<sub>1</sub>-, T<sub>2</sub>-weighted images, and about 52% in gradient echo axial images.

In conclusion, the staircase coil designed and fabricated during this study was found to be optimum in terms of performance with a conventional birdcage coil. Therefore, the staircase coil should be useful in experimental and clinical 1.5T MRI systems.

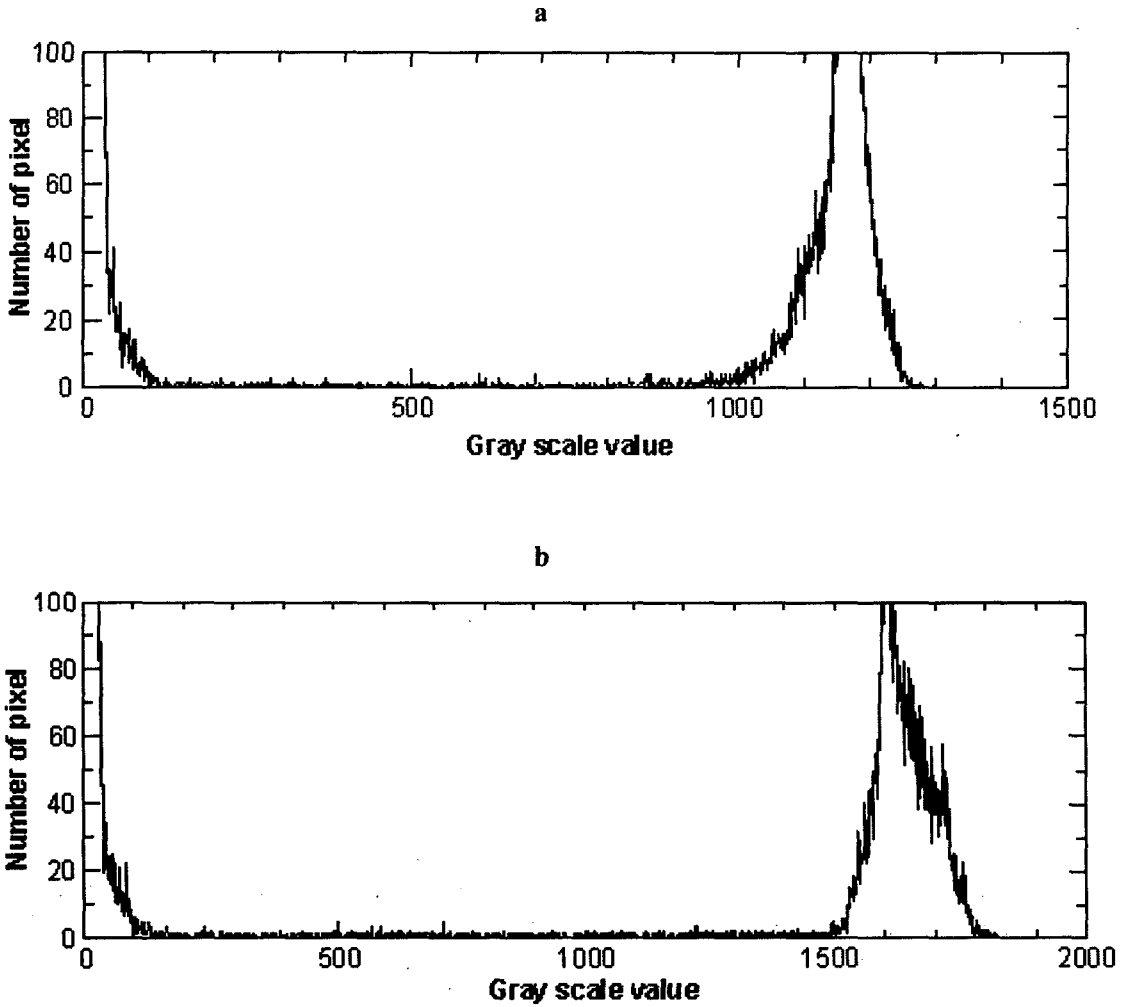


Fig. 3. Histogram of the axial phantom images acquired using the IDL program. a) Birdcage coil and b) staircase coil.





Fig. 4. T<sub>1</sub>-weighted sagittal images of the wrist joint that were acquired using a) a birdcage coil and b) a staircase coil.



Fig. 5. T<sub>2</sub>-weighted sagittal images of wrist joint that were acquired using a) a birdcage coil and b) a staircase coil.

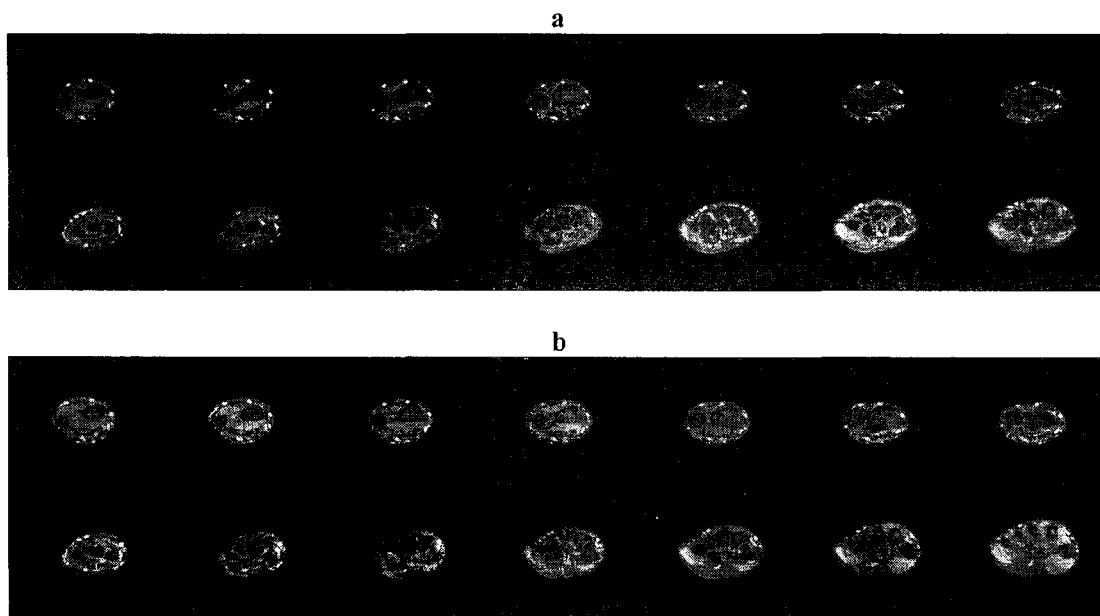


Fig. 6. Gradient echo axial images of wrist joint that were acquired using a) a birdcage coil and b) a staircase coil.

## REFERENCES

1. Cecil E. Hayes, William A. Edelstein, and John F. Schenck, Otward M. Mueller, and Matthew Eash, An efficient, highly homogeneous radiofrequency coil for whole-body NMR imaging at 1.5T. *J Magn Reson*, **63**, 622-628 (1985).
2. James Tropp, The theory of the bird-cage resonator. *J Magn Reson*, **82**, 51-62 (1989).
3. Jianming Jin, Gray Shen, and Thomas Perkins, On the field inhomogeneity of a Birdcage Coil. *Magn Reson Med*, **32**, 418-422 (1994).
4. J. Bruce Kneeland and James S. Hyde, High-resolution MR imaging with local coils. *Radiology*, **171**, 1-7 (1989).
5. F. David Doty, George Entzminger Jr., and Cory D. Hauck, Error-tolerant RF Litz coils for NMR/MRI. *J Magn Reson*, **140**, 17-31 (1999).
6. Claasen-Vujcic T., Borsboom H. M., and Gaykema H. J. G. Gaykema, Toon Mehlkopf, Transverse low-field RF coils in MRI. *Magn Reson Med*, **36**, 111-116 (1996).

7. Han Wen, Andrew S. Chesnick, and Robert S. Balaban, The design and test of a new volume coil for high field imaging. *Magn Reson Med*, **32**, 492-498 (1994).
8. Thomas Vullo, Raymond T. Zipagan, and Romeo Pascone, Joseph P. Whalen, and Patrick T. Cahill, Experimental design and fabrication of birdcage resonators for magnetic resonance imaging. *Magn Reson Med*, **24**, 243-252 (1992).
9. Yan Xu, and Pei Tang, Easy fabrication of a tunable high-pass birdcage resonator. *Magn Reson Med*, **38**, 168-172 (1997).
10. Julia Gasson, Ian R. Summers, and Martin E. Fry, and William Vennart, Modified birdcage coils for targeted imaging. *J Magn Reson*, **13**, 1003-1012 (1995).
11. Fujita H., Braum W. O., and Morich M. A. Novel quadrature birdcage coil for a vertical  $B_0$  field open MRI system. *Magn Reson Med*, **44**, 633-640 (2000).
12. Shizhe Li, Christopher M. Collins, and Bernard J. Dardzinski, Chih-liang Chin, Michael B. Smith, A method to create an optimum current distribution and homogeneous  $B_1$  field for elliptical birdcage coils. *Magn Reson Med*, **37**, 600-608 (1997).
13. David C. Alsop, Thomas J. Connick, and Gabor Mizsei, A spiral volume coil for improved RF field homogeneity at high static magnetic field strength. *Magn Reson Med*, **40**, 49-54 (1998).
14. Gray X. Shen, J. F. Wu, and Fernando E. Boada, Keith R. Thulborn, Experimentally verified, theoretical design of dual-tuned, low-pass birdcage radiofrequency resonators for magnetic resonance imaging and magnetic resonance spectroscopy of human brain at 3.0 tesla. *Magn Reson Med*, **41**, 268-275 (1999).
15. C. N. Chen, D. I. Hoult, and V. J. Sank, Quadrature detection coils - A further improvement in sensitivity." *J Magn Reson*, **54**, 324-327 (1983).